11-1-2007

# Calcium-dependent fast depolarizing afterpotentials in vasopressin neurons in the rat supraoptic nucleus

Ryoichi Teruyama
*University of Tennessee*

William E. Armstrong
*University of Tennessee*



## Recommended Citation

Teruyama, R., & Armstrong, W. (2007). Calcium-dependent fast depolarizing afterpotentials in vasopressin neurons in the rat supraoptic nucleus. *Journal of Neurophysiology, 98* (5), 2612-2621. https://doi.org/10.1152/jn.00599.2007

*J Neurophysiol* 98: 2612–2621, 2007.
First published August 22, 2007; doi:10.1152/jn.00599.2007.

# Calcium-Dependent Fast Depolarizing Afterpotentials in Vasopressin Neurons in the Rat Supraoptic Nucleus

**Ryoichi Teruyama and William E. Armstrong**
*Department of Anatomy and Neurobiology, University of Tennessee, Health Science Center, Tennessee*

Submitted 25 May 2007; accepted in final form 16 August 2007

**Teruyama R, Armstrong WE.** Calcium-dependent fast depolarizing afterpotentials in vasopressin neurons in the rat supraoptic nucleus. *J Neurophysiol* 98: 2612–2621, 2007. First published August 22, 2007; doi:10.1152/jn.00599.2007. Oxytocin (OT) and vasopressin (VP) synthesizing magnocellular cells (MNCs) in the supraoptic nucleus (SON) display distinct firing patterns during the physiological demands for these hormones. Depolarizing afterpotentials (DAPs) in these neurons are involved in controlling phasic bursting in VP neurons. Our whole cell recordings demonstrated a $Cs^+$-resistant fast DAP (fDAP; decay tau = ~200 ms), which has not been previously reported, in addition to the well-known $Cs^+$-sensitive slower DAP (sDAP; decay tau = ~2 s). Immunoidentification of recorded neurons revealed that all VP neurons, but only 20% of OT neurons, expressed the fDAP. The activation of the fDAP required influx of $Ca^{2+}$ through voltage-gated $Ca^{2+}$ channels as it was strongly suppressed in $Ca^{2+}$-free extracellular solution or by bath application of $Cd^{2+}$. Additionally, the current underlying the fDAP ($I_{fDAP}$) is a $Ca^{2+}$-activated current rather than a $Ca^{2+}$ current per se as it was abolished by strongly buffering intracellular $Ca^{2+}$ with BAPTA. The *I-V* relationship of the $I_{fDAP}$ was linear at potentials less than −60 mV but showed pronounced outward rectification near −50 mV. $I_{fDAP}$ is sensitive to changes in extracellular $Na^+$ and $K^+$ but not $Cl^-$. A blocker of $Ca^{2+}$-activated nonselective cation (CAN) currents, flufenamic acid, blocked the fDAP, suggesting the involvement of a CAN current in the generation of fDAP in VP neurons. We speculate that the two DAPs have different roles in generating after burst discharges and could play important roles in determining the distinct firing properties of VP neurons in the SON neurons.

## INTRODUCTION

The secretion of neurohormones into the circulation largely depends on the pattern of neuronal activity of the synthesizing neurons. The neurohypophysial hormones vasopressin (VP) and oxytocin (OT) are synthesized in magnocellular cells (MNCs) within the supraoptic nuclei (SON), and these two neuron types show distinct firing patterns when physiological demands for their hormones are high. Preceding each milk ejection in lactating rats, the firing pattern in OT neurons changes dramatically, characterized by a short (2–4 s), high-frequency (≤80 Hz) burst of action potentials (Poulain and Wakerley 1982). In contrast, VP neurons respond to hyperosmolality (Brimble and Dyball 1977) and hypovolemia (Harris et al. 1975) by increasing their firing rate and adopting a phasic firing pattern comprising alternating periods of activity (7–15 Hz) and silence, each lasting tens of seconds. The release of VP is maximized by stimulation patterns mimicking phasic firing (Cazalis et al. 1985; Dutton, and Dyball 1979). The emergence of these firing patterns is therefore an important part of the response of MNCs during their hormonal demands.

The firing pattern of a neuron is generally a result of the interaction between synaptic and intrinsic membrane properties of the neuron. The depolarizing afterpotential (DAP) is an intrinsic membrane property of MNCs, originally observed after a single spike or a brief spike train in a subpopulation of MNCs (Andrew and Dudek 1983). Summation of DAPs induces a plateau potential that underlies the burst of action potentials in phasic neurons (Andrew and Dudek 1984a; Ghamari-Langroudi and Bourque 1998) and is found in most VP neurons and a minority of OT neurons (Armstrong et al. 1994; Smith and Armstrong 1993). However, DAPs may also play a role in the short bursting activity in OT neurons as their expression in these neurons is increased during pregnancy and lactation (Stern and Armstrong 1996; Teruyama and Armstrong 2002).

Although, there is strong agreement that DAPs in MNCs are triggered by $Ca^{2+}$ influx during spikes (Andrew and Dudek 1984a; Greffrath et al. 1998; Li and Hatton 1997a; Smith and Armstrong 1993), their ionic basis is not fully understood. One study suggested that DAPs may result from the $Ca^{2+}$-dependent reduction of a resting $K^+$ conductance (Li and Hatton 1997b). In that study, DAPs were attenuated by tetrodotoxin (TTX) or tetraethyl ammonium (TEA) but were relatively insensitive to external $Cs^+$. In other studies, DAPs were not blocked by TTX (Andrew 1987) or TEA (Greffrath et al. 1998), but they were blocked by external $Cs^+$ (Ghamari-Langroudi and Bourque 1998). More recent work suggested the involvement of a $Ca^{2+}$-activated nonselective cation (CAN) channel because the CAN channel blocker, flufenamic acid (FFA), reversibly inhibited DAPs and phasic firing in MNCs (Ghamari-Langroudi and Bourque 2002). These disparate results may imply that multiple currents underlie DAPs. Recently, when blocking the apamin-sensitive medium AHP (mAHP), we unmasked a DAP that was faster than that typically described in MNCs. The present study was conducted to investigate the properties of this fast DAP in MNCs and has previously been published in abstract from (Teruyama and Armstrong 2005b, 2006).

## METHODS

### *Animals and slice preparation*

Brain slices containing the SON were prepared from random cycling, virgin female adult rats (180–210 g body wt; Sprague-

Address for reprint requests and other correspondence: R. Teruyama, Dept. of Anatomy and Neurobiology, University of Tennessee, Health Science Center, 855 Monroe Ave., TN 38163 (E-mail: rteruyam@utmem.edu).

The costs of publication of this article were defrayed in part by the payment of page charges. The article must therefore be hereby marked "*advertisement*" in accordance with 18 U.S.C. Section 1734 solely to indicate this fact.

  

Dawley, Harlan Laboratories, Indianapolis, IN). The rats were deeply anesthetized with sodium pentobarbital (50 mg/kg ip) and perfused through the heart with a sucrose solution (an artificial cerebrospinal fluid (ACSF) solution (see following text) in which NaCl was replaced by an equiosmolar amount of sucrose). The brains were removed and sliced in the coronal plane at a thickness of 250 $\mu$m in the ice-cold sucrose solution. Slices were maintained in ACSF, which was bubbled continuously with 95% $O_2$-5% $CO_2$, containing (in mM) 124 NaCl, 3 KCl, 2.0 $CaCl_2$, 1.3 $MgCl_2$, 1.24 $NaH_2PO_4$, 25 $NaHCO_3$, 0.2 ascorbic acid, and 10 D-glucose (pH 7.4). Slices were stored at room temperature prior to recording. Animal procedures were performed under protocols approved by the Institutional Animal Care and Use Committee at University of Tennessee.

### *Electrophysiology*

Whole cell patch-clamp recordings were obtained with an Axon 200B amplifier (Axon Instruments, Foster City, CA). Traces were acquired digitally at 20 kHz and filtered at 5 kHz with a Digidata 1320A (Axon Instruments) in conjunction with pClamp 9 software (Axon Instruments). Axograph 4.9 (Axon Instruments) was used to analyze the recordings. The current-voltage relationships were analyzed using Igor Pro Carbon 4.07 (WaveMetrics, Lake Oswego, OR). Averaged data are presented as the means ± SE, where $n$ is the number of cells. Statistically significant difference between means was set to $P < 0.05$, using paired Student's $t$-test, unless otherwise stated.

For analyzing the tail currents, K- and Cs-gluconate pipette solutions were used. The K-gluconate pipette solution consisted of (in mM) 135 K-gluconate, 2 $MgCl_2$, 10 HEPES, 10 phosphocreatine, 10 myo-inositol (no phosphate), 0.1 EGTA, 0.4 GTP (Na), and 2 ATP (Mg). The pipette solutions were adjusted to a pH of 7.3 with KOH. In some experiments, bis-(*o*-aminophenoxy)-*N,N,N′,N′*-tetraacetic acid (BAPTA, 10 mM) was added to this pipette solution. The Cs-gluconate pipette solution consisted of (in mM) 100 CsOH, 100 D-gluconic acid, 10 HEPES, 2 $MgCl_2$; 2 ATP (Mg); 0.4 GTP (Na), 10 phosphocreatine, 10 myo-inositol (no phospate), and 0.1 EGTA. The pipette solutions were adjusted to a pH of 7.3 with HCl. Phosphocreatine was included because "rundown" of $Ca^{2+}$ currents was effectively reduced by such inclusion to allow regeneration of ATP (Foehring and Armstrong 1996). Myo-inositol was added to prevent possible rundown of the fDAP because phosphatidylinositol 4,5-bisphosphate plays a central role in the activation of several CAN channels (Rohacs et al. 2005). Both pipette solutions contained 0.2% biocytin (Sigma, St. Louis, MO) to identify the patched cell (see *Immunocytochemistry*). Patch electrodes were drawn from borosilicate capillary glass tubing (G150TF-3, Warner Instruments, Hamden, CT) to have resistances of 4–8 MΩ when filled with these pipette solutions. The calculated liquid junction potential (LJP) for the various external solutions and Cs-gluconate internal ranged from +12.4 to +14.8 mV. For the K-gluconate internal solution, the LJPs ranged from +9.2 to +12.2 mV, The maximal difference within any one experiment involving a solution exchange was +3 mV. The data presented were not corrected for LJPs. To isolate the current underlying the fast DAP, $Cs^+$ (5 mM), apamin (100 nM), and tetrodotoxin (TTX; 500 nM) were added to the ACSF unless otherwise stated. Picrotoxin (100 $\mu$M) and 6,7-dinitro-quinoxaline-2,3(1H,4H)-dione (DNQX, 10 $\mu$M) were also added to ACSF to suppress the synaptic activity. For voltage-clamp recordings with K-gluconate pipette solution, tetraethylamonium chloride (TEA-Cl; 10 mM) and 4-aminopyridine (4-AP; 10 mM) were added to, and 20 mM NaCl was subtracted from, the ACSF to suppress $K^+$ conductances. To create a $Na^+$-deficient solution, NaCl was replaced by an equiosmolar amount of sucrose. To create a $Cl^-$-deficient solution, NaCl was replaced by an equiosmolar amount of Na-thiocyanate. All the current-clamp recordings were conducted with the K-gluconate pipette solution. In some cases, the following compounds were added to the ACSF and perfused through the recording chamber: $CdCl_2$ (400 $\mu$M), flufenamic acid (10 $\mu$M), ruthenium red (1–10 $\mu$M), capsazepine (10 $\mu$M), SKF 96365 (10–100 $\mu$M; Tocris, Ellisville, MO), and U-50488 (10 $\mu$M: Tocris). All chemicals were purchased from Sigma unless otherwise stated. All extracellular media were saturated with 95% $O_2$-5% $CO_2$, with a pH of 7.3–7.4, had an osmolality of 290–300 mosM/kg $H_2O$, and were warmed to 33°C during the recording.

### *Immunocytochemistry*

After recording, the slices were fixed with 4% paraformaldehyde and 0.2% picric acid in phosphate-buffered saline (PBS) at 4°C for at least overnight and processed for double-immunofluorescence labeling. The anti-VP-neurophysin antiserum is a rabbit polyclonal provided by A. Robinson and was used at a 1:20,000 dilution. The anti-OT-neurophysin antibody (PS36) is a mouse monoclonal antibody provided by H. Gainer (National Institutes of Health) and was used at a 1:500 dilution. All antibodies and other labeling reagents were dissolved in PBS containing 0.5% Triton X-100. The slices were incubated 48–72 h at 4°C followed by the incubation in a cocktail of secondary antibodies and 7-amino-4-methylcoumarin-3-acetic acid (avidin-AMCA; Vector Labs, Burlingame, CA) 4–6 h at room temperature. The secondary antibodies used were fluorescein isothiocyanate (FITC)-conjugated goat anti-rabbit (Vector Labs) and Alexa Fluor 594-conjugated goat anti-mouse IgG (Invitrogen, Eugene, OR). Avidin-AMCA was used to visualize the recorded cells. Neurons were considered as either OT or VP types only if positive staining of one antibody was complemented by a negative reaction with the other (Fig. 1).

## RESULTS

### *$Cs^+$-sensitive and -resistant DAPs are both present in MNCs*

Prominent DAPs were observed following a train of action potentials in a subpopulation of MNCs. Among those cells expressing DAPs, repetitive single action potentials evoked by intracellular current injections (20 × 5 ms depolarizing pulses, 100–250 pA, 20 Hz) generated a DAP after the AHPs (Fig. 2*A*). The AHP generated with this protocol appeared to be mostly the medium AHP (mAHP) from its decay time course (~500 ms). The current underlying the mAHP is mediated by the small-conductance $Ca^{2+}$-activated $K^+$ channels (SK channels) in MNCs because it is blocked by bee venom apamin, a known blocker of SK channels (Armstrong et al. 1994; Bourque and Brown 1987; Greffrath et al. 1998; Kirkpatrick and Bourque 1996; Teruyama and Armstrong 2005a). As expected, bath application of apamin (100 nM) strongly suppressed the

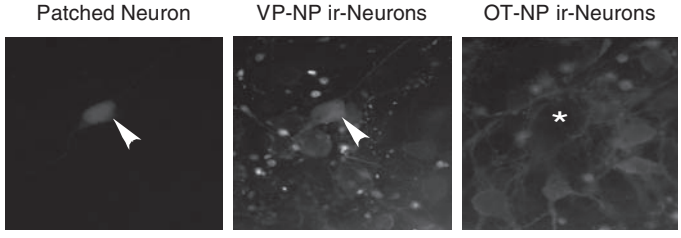


FIG. 1. Immunocytochemical identification of cell types in magnocellular cells (MNCs) from supraoptic nucleus (SON). The patched neuron was filled with biocytin and visualized by 7-amino-4-methylcoumarin-3-acetic acid (AMCA)-conjugated avidin (arrowhead, *left*). The tissue was also labeled for vasopressin (VP) and oxytocin (OT) neurophysins (NP) by immunofluorescence using fluorescein isothiocynate and Alexa Fluor 594-conjugated secondary antibodies, respectively. The recorded cell was immunoreactive to VP-NP (arrowhead, *middle*) but not to OT-VP (*, *right*).

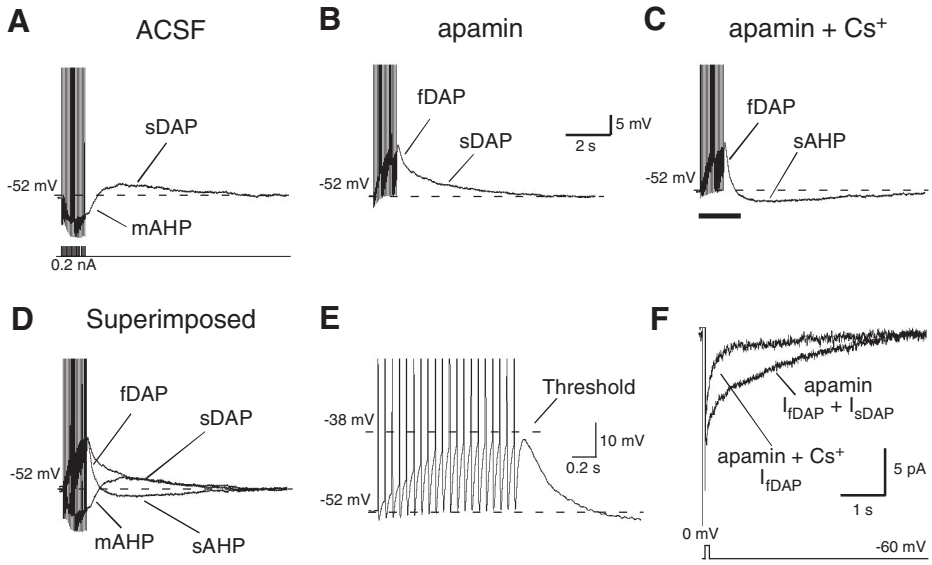


FIG. 2. $Cs^+$-sensitive and -resistant depolarizing afterpotentials (DAPs) in MNCs. Afterpotentials in a MNC were generated by a train of action potentials evoked by intracellular current injections (20 × 5 ms depolarizing pulses, 100–250 pA, 20Hz). *A*: in artificial cerebrospinal fluid (ACSF), the train of action potentials was followed by a distinct medium afterhyperpolarization (mAHP) that was subsequently followed by the slow DAP (sDAP). *B*: bath application of apamin (100 nM) completely blocked the mAHP and unmasked the presence of the fast DAP (fDAP), which was followed by the sDAP. *C*: additional application of $Cs^+$ (5 mM) blocked the sDAP that revealed the sAHP. *D*: superimposed traces of *A–C* illustrate the temporally overlapping, multiple afterpotentials. *E*: expanded portion of the trace in *C* (indicated by underline) revealed that the onset of the fDAP occurred after the 1st action potential and its amplitude increased with each subsequent action potential until a plateau was reached after 12 spikes. *F*: inward tail current thought to be underlying the DAPs ($I_{DAPs}$) was generated by 50 ms steps to 0 mV from a holding potential of −60 mV. Tail currents with similar time courses as the fast and slow DAPs were obtained and the application of 5 mM $Cs^+$ blocked only $I_{sDAP}$.

mAHP, enhanced the DAP, and shifted its peak to the left (Fig. 2*B*). It has been known that $Cs^+$ blocks the DAP in MNCs (Ghamari-Langroudi and Bourque 1998). However, in the presence of apamin, bath application of $Cs^+$ (5 mM) blocked only a slower part of the DAP and not the peak (Fig. 2*C*). Inhibition of the slow part of the DAP with $Cs^+$, in turn, revealed the presence of the slow AHP (sAHP) described previously in MNCs (Ghamari-Langroudi and Bourque 2004; Greffrath et al. 1998; Teruyama and Armstrong 2005a). The time course of the faster part of the DAPs could not be observed easily with this protocol unless the mAHP and the slower part of the DAPs were both suppressed. Because the time course of the $Cs^+$-resistant DAP is faster than the $Cs^+$-sensitive DAP, we refer to them as fast DAP (fDAP) and slow DAP (sDAP), respectively. The superimposed images from Fig. 2, *A–C* (Fig. 2*D*) illustrate the presence of multiple, temporally overlapping afterpotentials in the MNC. It is clear that time courses of the mAHP and sAHP overlap considerably with those of the fDAP and sDAP, respectively.

The fDAP showed strong activity dependence. More detailed observation in the expanded portion of the trace during repetitive spike activation (Fig. 2*E*) revealed that the onset of the fDAP was seen after the first action potential and its amplitude continued to increase with each subsequent action potential until a plateau was reached after ~15 spikes.

The inward tail currents thought to underlie the DAP ($I_{DAP}$) were generated by 50 ms steps to 0 mV from the holding potential of −60 mV in the presence of apamin (100 nM) in the bathing solution (Fig. 2*F*). Tail currents with time courses similar to the fDAP and sDAP were obtained. Bath application of 5 mM $Cs^+$ blocked only the slow part of the $I_{DAP}$, similar to its effect on the sDAP in current clamp (Fig. 2*F*). The time course of the $I_{fDAP}$ was fitted with a single-exponential function with a time constant of decay of 283.0 ± 12.7 ms ($n = 29$) for a pulse duration of 50 ms at a holding potential of −60 mV.

Because the fDAP showed strong activity dependence, the dependence of the $I_{fDAP}$ on the duration of depolarizing steps was evaluated in voltage clamp. These steps would allow a progressive increase in $[Ca^{2+}]_i$. This protocol was chosen over mimicking spikes in current clamp because it better isolated the fDAP from the sAHP, which increases with spike number during a train, because it provides a better space clamp than transient depolarizations that would be heavily filtered, and because the activity dependence in current clamp is heavily dependent on spike frequency. The amplitude of $I_{fDAP}$ increased with the duration of the stimulus, and the maximum amplitude $I_{fDAP}$ reached with the pulse duration of 150 ms (Fig. 3*A; n* = 5). The relationship between peak $I_{fDAP}$ amplitude and pulse duration was fitted with a single-exponential function with a time constant of ~100 ms ($n = 4$; Fig. 3*B*).

Under our recording conditions, fDAPs were seen in the vast majority of VP neurons. Only 1 in 69 immunolabeled VP neurons failed to express fDAP. In contrast, only 13 of 65 (20%) immunolabeled OT neurons expressed the fDAP. To study the fDAP and its underlying current, we analyzed the recordings exclusively from the immunolabeled VP neurons. To isolate the fDAP, experiments were conducted in the presence of apamin (100 nM) and $Cs^+$ (5 mM) unless otherwise stated.

### *$Ca^{2+}$ dependence of the fDAP*

Although the mechanisms underlying the DAP in MNCs are controversial, previous studies agree they are $Ca^{2+}$ dependent (Andrew and Dudek 1984b; Ghamari-Langroudi and Bourque 1998; Li and Hatton 1997a). $Ca^{2+}$ influx appeared to be an

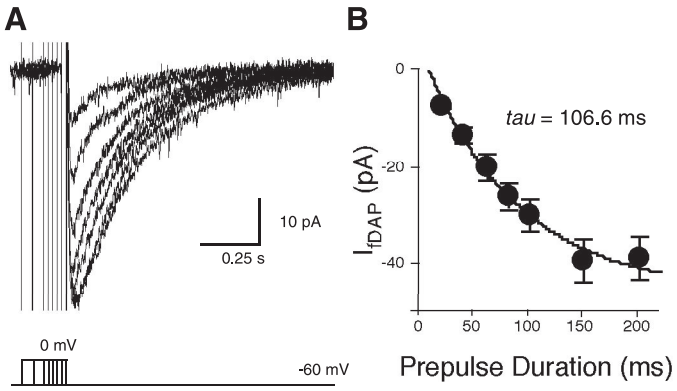


FIG. 3. Dependence of the $I_{fDAP}$ on the duration of the depolarizing pulses. *A*: amplitude of the $I_{fDAP}$ increased with stimulus duration. *B*: relationship between amplitude of the peak current and pulse duration could be fitted with a single-exponential function. The amplitude reached a maximum value at 150 ms of duration ($n = 4$).

important determinant for the activation of the fDAP as well. Lowering extracellular $Ca^{2+}$ concentration reversibly inhibited the fDAP (Fig. 4*A; n* = 6). A similar effect on $I_{fDAP}$ was observed when $Ca^{2+}$ channels were blocked by bath application of 400 $\mu$M $Cd^{+}$ (Fig. 4*B; n* = 5). These results indicate that the fDAP is also $Ca^{2+}$ dependent.

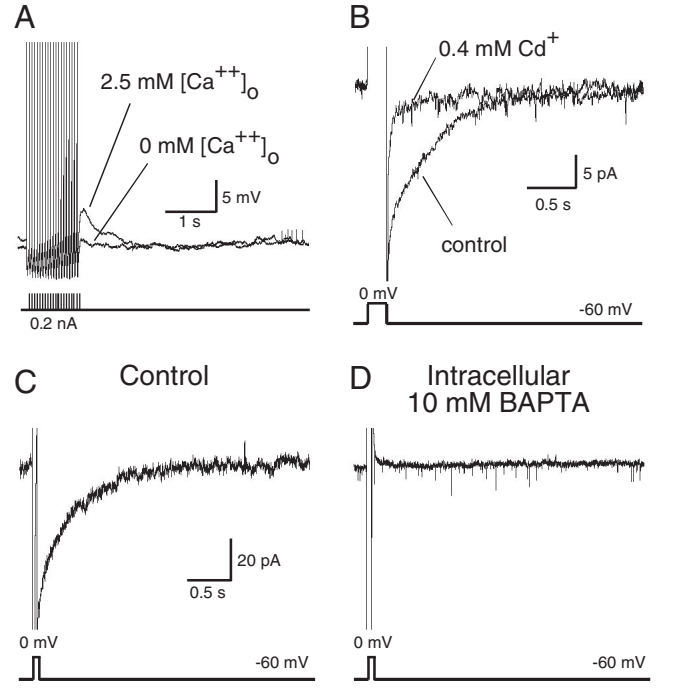


FIG. 4. $Ca^{2+}$ dependency of the fDAP and its underlying current. *A*: reduction of external $Ca^{2+}$ concentration abolished the fDAP. *B*: application of a $Ca^{2+}$ channel blocker, $Cd^{+}$ (0.4 mM), blocked the $I_{fDAP}$. *C*: $I_{fDAP}$ was always observed with the normal pipette solution. *D*: $I_{fDAP}$ was never observed when intracellular $Ca^{2+}$ was buffered with 10 mM bis-(*o*-aminophenoxy)-*N,N,N′,N′*-tetraacetic acid (BAPTA, 7 cells tested), indicating the $I_{fDAP}$ is not a $Ca^{2+}$ current, but a $Ca^{2+}$- dependent current. The fDAP in *A* was generated by a train of 20 action potentials evoked by brief stimulus pulses (0.2 nA, 5 ms, 20 Hz) in the presence of $Cs^{+}$ (5 mM) and apamin (100 nM). The $I_{fDAP}$ in *B–D* were generated by a 50-ms depolarizing voltage step to 0 mV from the holding potential of −60 mV, then returned to −60 mV in the presence of $Cs^{+}$ (5 mM), 4-aminopyridine (4-AP, 10 mM), TEA (10 mM), apamin (100 nM), and TTX (500 nM), with K-gluconate intracellular solution.

To distinguish between $I_{fDAP}$ as a $Ca^{2+}$-activated current versus a $Ca^{2+}$ current per se, recordings were made with high intracellular buffering of $Ca^{2+}$. If the underlying current is a $Ca^{2+}$ current, the $I_{fDAP}$ should be observed despite strongly buffering $Ca^{2+}$ with intracellular BAPTA (10 mM). As illustrated in Fig. 4, *C* and *D,* the $I_{fDAP}$ was never observed in the recordings with an intracellular solution containing BAPTA ($n = 9$). These results showed that the $I_{fDAP}$ is probably not a voltage-gated $Ca^{2+}$ current but rather is a $Ca^{2+}$-activated current.

### *$Na^{+}$ influx through TTX-sensitive channel is not required for the fDAP production*

Because the application of TTX reduced $I_{DAPs}$ in MNCs in the study of Li and Hatton (1997b), the possibility that the fDAP is a result of TTX-sensitive $Na^{+}$ channels was evaluated. A train of action potentials was evoked by a 200 ms stimulus pulse (0.2 nA) to generate a fDAP in the presence of apamin (100 nM) and $Cs^{+}$ (5 mM). Subsequent bath application of TTX (0.5 $\mu$M) blocked sodium spikes and a presumptive persistent $Na^{+}$ current (not shown), but the fDAP evoked by calcium spikes remained constant (Fig. 5; $n = 8$). Therefore the activation of TTX-sensitive sodium channels is not required for generation of the fDAP in VP neurons.

### *Current-voltage relationship of the $I_{fDAP}$*

The current-voltage relationship of the $I_{fDAP}$ was examined at various holding potentials under voltage clamp. In this experiment, activation of $I_{fDAP}$ was conducted in VP neurons filled with $Cs^{+}$-gluconate pipette solution. The tail current thought to underlie the fDAP was evoked by a 50 ms depolarizing voltage step to 0 mV from the holding potential of −60 mV, then returned to different membrane potentials (Fig. 6*A*). To isolate this $Ca^{2+}$-dependent inward current from the influence of other voltage-dependent currents, traces taken without the conditioning pulse (used to produce $Ca^{2+}$ influx) were subtracted from the traces obtained from those with test pulses (Fig. 6, *A* and *B*). The *I-V* relationship of the $I_{fDAP}$ was characterized by a relatively linear relation between −90 and −50 mV and pronounced outward rectification above −50 mV (Fig. 6*C*). The outward rectification suggested that the channel is permeable to $Cs^{+}$ and is probably regulated by membrane voltage as well as $Ca^{2+}$, although a more thorough characterization of voltage dependence would require a more extended

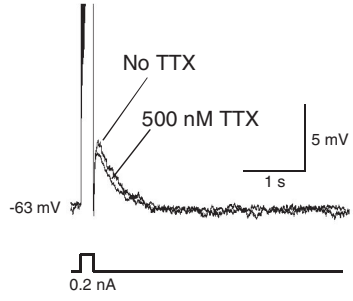


FIG. 5. The effect of TTX on the fDAP. fDAPs were generated by evoking action potentials by applying 200 ms square current injection in the presence of $Cs^{+}$ (5 mM) and apamin (100 nM), while the membrane potential was held at −63 mV. Application of TTX (500 nM) blocked $Na^{+}$ spikes, but failed to block the fDAP after strong membrane potential depolarization ($n = 8$).

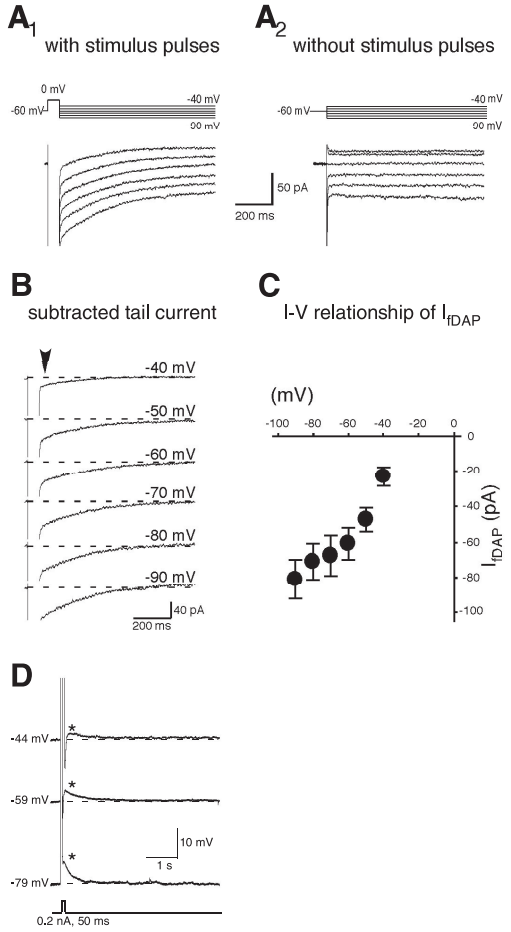


FIG. 6. The currrent-voltage (*I-V*) relationship of the $I_{fDAP}$. *A1*: tail current was generated by a 50 ms depolarizing voltage step to 0 mV from a holding potential of −60 mV, then returned to different test membrane potentials from −90 to −40 mV. *A2*: control traces were obtained without the conditioning depolarizing step. *B*: to isolate the $Ca^{2+}$- dependent inward current of $I_{fDAP}$, control traces (*A2*) were subtracted from test traces (*A1*). ▼, where current amplitudes were measured. *C*: *I-V* relationship was relatively linear between −90 and −50 mV but rectified outwardly above −50 mV, suggesting a voltage dependence of the current. These recordings were conducted with $Cs^+$-gluconate intracellular solution in the presence of extracellular $Cs^+$, apamin, and TTX (5 mM, 100 nM, and 500 nM, respectively). *D*: fDAPs were generated by evoking action potentials with a 50 ms square pulse in the presence of apamin (100 nM), $Cs^+$ (5 mM), TEA (10 mM), and TTX (500 nM). The amplitudes of the fDAP became larger when the holding potential was hyperpolarized, complementing the *I-V* relationship in voltage clamp.

*I-V* curve in complete isolation of other currents. The reversal potential was estimated to be between −30 and −40 mV from extrapolation of the *I-V* curve. This apparent reversal potential was not near that of any major intracellular ion species, suggesting a current carried by a mixture of cations. When the fDAP was generated by evoking action potentials with a 50 ms stimulus pulse in the presence of apamin, $Cs^+$, and TTX (100 nM, 5 mM, and 500 nM, respectively) from various holding membrane potentials, the amplitude of the fDAP decreased as membrane potential was depolarized (Fig. 6*D*). This result complements the finding that the amplitude of the $I_{fDAP}$ became smaller when the holding potential was depolarized.

### *Ionic dependence of the current underlying fDAP*

Because a mixed cation current was suggested as the ionic basis of the current, we tested $Na^+$ permeability by lowering $[NaCl]_o$ to 27 mM in VP neurons filled with $Cs^+$-gluconate-filled pipettes. The Nernst equation indicated that this treatment would shift $E_{Na^+}$ negative by 46 mV and $E_{Cl^-}$ positive by 87 mV. As shown in Fig. 7, reduction of the $[NaCl]_o$ in the bathing solution resulted in significant reduction in the amplitude of $I_{fDAP}$ at potentials between −90 and −50 mV ($n = 5$; $P < 0.05$). This suggests the involvement of $Na^+$ in generation of fDAP.

To test whether $I_{fDAP}$ is also carried by $K^+$ ions, the effect of raising extracellular $K^+$ concentration to 10 mM from control of 2.5 mM was examined in VP neurons filled with K-gluconate pipette solution. This treatment would shift $E_{K^+}$ positive by 37 mV (Nernst equation). To minimize the effect of voltage-dependent $K^+$ conductances, TEA and 4-AP (10 mM each) were added along with apamin, $Cs^+$, and TTX (100 nM, 5 mM, and 500 nM, respectively) in the bathing solution. Despite these treatments, a transient outward current opposing the $I_{fDAP}$ appeared at potentials above −50 mV (indicated in Fig. 8*A*), indicating the presence of a probable $K^+$ current (which was blocked by the internal $Cs^+$ in the previous experiment). However, the amplitudes obtained for plotting the *I-V* relationship were taken from the point (indicated in arrowheads) where the outward current subsided, therefore minimizing contamination, and in control solution, produced an *I-V* curve similar to that when $Cs^+$ was used intracellularly to block other $K^+$ currents in the experiments testing for $Na^+$ dependence (Fig. 7). Raising the extracellular concentration of $K^+$ significantly increased amplitudes of the $I_{fDAP}$ ($n = 6$; $P < 0.05$) and shifted its reversal potential in the depolarizing direction. Thus $K^+$ also contributes to the amplitude of the $I_{fDAP}$.

$Ca^{2+}$-activated $Cl^-$ currents have been reported to mediate depolarizing afterpotentials in other cell types, such as dorsal root ganglion, spinal cord, and autonomic neurons (reviewed in Hartzell et al. 2005). In VP neurons filled with our K-gluconate pipette solution, $E_{Cl^-}$ would be approximately −63 mV. Opening of $Ca^{2+}$-activated $Cl^-$ channels could contribute to depolarization when the membrane potential is more positive than

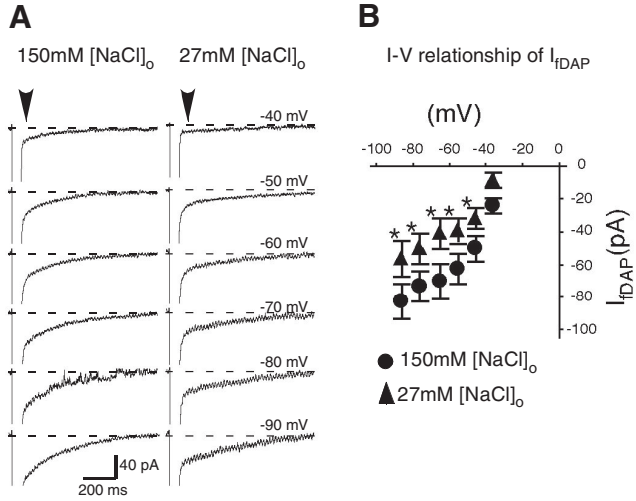


FIG. 7. Effect of lowering $[Na^+]_o$ on $I_{fDAP}$. *A*: $I_{fDAP}$ at membrane potentials from −90 to −40 mV was obtained by the subtraction method described in the previous figure. *B*: plotted *I-V* shows that lowering $[Na^+]_o$ significantly decreases the amplitude of the $I_{fDAP}$ throughout the voltage range −90 to −50 mV ($n = 5$; $P < 0.05$).

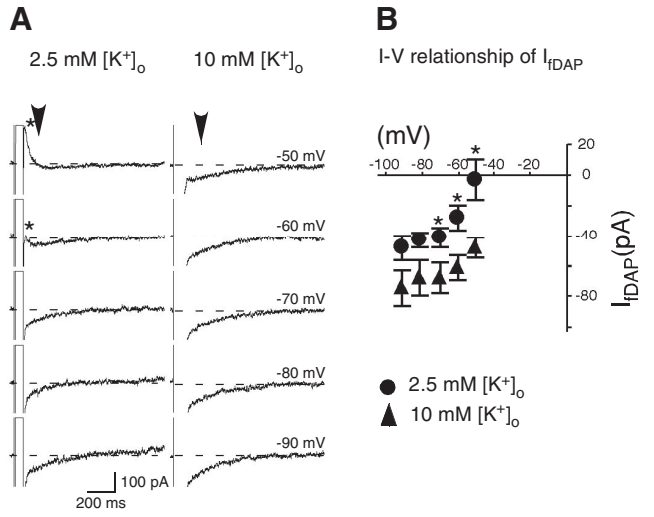


FIG. 8. Effect of raising $[K^+]_o$ on $I_{fDAP}$. *A*: $I_{fDAP}$ at potentials between −90 and −40 mV was obtained by the subtraction method described in Fig. 7 at 2 different concentrations of extracellular $K^+$. Recordings with $K^+$ gluconate pipette solution. *B*: *I-V* relationship of the $I_{fDAP}$ in normal and high $[K^+]_o$. Raising $[K^+]_o$ to 10 mM from 2.5 mM significantly increased the amplitude of $I_{fDAP}$ from −70 to −40 mV ($n = 6$; $P < 0.05$), but the rectification at −50 and −40 mV was still apparent. The recordings were conducted in the presence of $Cs^+$ (5 mM), 4-AP (10 mM), TEA (10 mM), apamin (100 nM), and TTX (500 nM). Arrowheads, points where the amplitude of the tail currents was measured.

$E_{Cl}^-$. The possibility was examined by replacing extracellular chloride with equiosmolar thiocyanate. As illustrated in Fig. 9, reducing extracellular chloride from 127.5 to 2.5 mM did not change the $I_{fDAP}$, even at membrane potentials negative to $E_{Cl}$. Collectively, the data in Figs. 4-9 strongly suggest the involvement of a $Ca^{2+}$-activated mixed cation current, carried mainly by $Na^+$ and $K^+$ ions, in the generation of fDAP in VP neurons.

### *Pharmacological characterization of fDAP*

Together, the previous results suggest that a $Ca^{2+}$-activated nonselective cation (CAN) channel is responsible for generation of the fDAP in VP neurons. Therefore the effects of the several blockers of cation channels on the fDAP were tested. A nonsteroidal antiinflammatory drug, flufenamic acid (FFA), has been reported to block two closely related $Ca^{2+}$-activated cation channels, the melastatin-related subfamily of transient receptor potential (TRP) channels (TRPM4 and TRPM5 channels) (Ullrich et al. 2005). As shown in Fig. 10*A,* bath application of FFA (100 $\mu$M) significantly and reversibly reduced the amplitude of fDAP by 69.7 ± 10.6% ($n = 4$; $P < 0.05$). The blockade of the DAP by FFA had a slow onset (~12 min) and reversed only slowly (~15 min) on washout.

Another family of TRP channels, TRP vanilloid type 1, 2, and 4 (TRPV1, TRPV2, and TRPV4) were reported to be expressed in VP neurons (Wainwright et al. 2004). Therefore the effect of a TRPV blocker, the inorganic polycationic dye ruthenium red (RuR), on fDAP was examined. Bath application of RuR, even at 10 $\mu$M concentration, did not significantly affect the amplitude of fDAP ($n = 4$; Fig. 10*B*). Moreover, capsazepine, a competitive antagonist of capsaicin at the TRPV1 channel (Dickenson and Dray 1991), did not affect the amplitude of fDAP ($n = 2$; Fig. 10*C*). These results suggest the generation of fDAP is not mediated by TRPV channels. In addition, SKF 96365, a commonly used cation channel blocker that blocks TRP canonical type 3 (TRPC3) (Zhu et al. 1998) and type 6 (TRPC6) (Boulay et al. 1997; Inoue et al. 2001; Tseng et al. 2004) channels, did not affect the amplitude of fDAP ($n = 4$; Fig. 10*D*), indicating that TRPC3 and TRPC6 channels are not involved in the generation of fDAP in VP neurons. Although U50488H is not a cation channel blocker but rather a synthetic κ-opioid receptor agonist, the effect of this compound on the fDAP was tested because both endogenous dynorphin and U50488H have been reported to inhibit DAPs and decrease burst duration in MNCs (Brown and Bourque 2004; Brown et al. 1999). However, as seen in Fig. 10*E,* bath application of U50488 did not affect the amplitude fDAP ($n = 3$). Thus like external $Cs^+$, *k*-receptor activation probably targets the sDAP, but not the fDAP, in VP neurons.

## DISCUSSION

### *Supraoptic VP neurons generate a fast DAP*

The present study demonstrated that essentially all VP neurons in the SON generate a $Ca^{2+}$-dependent fDAP following a train of action potentials, whereas only minority of OT neurons expressed this afterpotential. Many studies have attempted to elucidate the mechanisms underlying DAPs in MNCs with disparate results. It has been suggested that discrepancies between labs may arise from the multiple mechanisms underlying the expression of DAPs in MNCs (Ghamari-Langroudi and Bourque 2002; Li and Hatton 1997b). Most previous studies of DAPs in MNCs were done in the presence of multiple overlapping voltage- and $Ca^{2+}$-dependent currents. Results will likely be biased to mechanisms that can be observed best under particular experimental conditions. Activation of each afterpotential may thus differ between experimental conditions (e.g., patch-clamp or sharp electrode experiments). For example, Li and Hatton (1997b) suggested that the DAP may result from the $Ca^{2+}$-dependent reduction of a resting $K^+$ conductance. The DAP in that study was attenuated by TTX or TEA and insensitive to external $Cs^+$. In contrast, DAPs in other studies were not blocked by TTX (Andrew

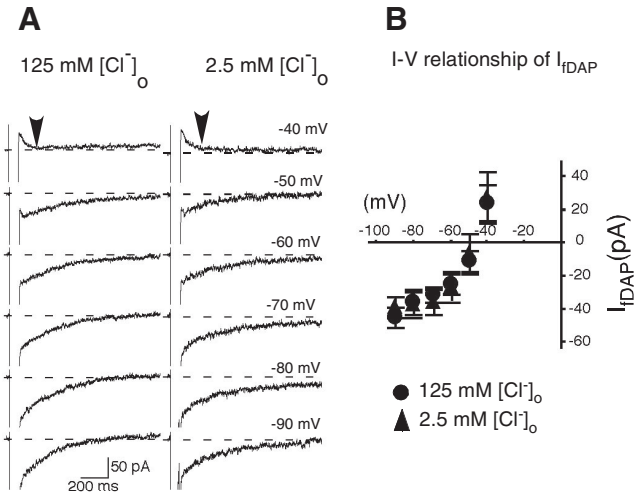


FIG. 9. Effect of lowering $[Cl^-]_o$ on $I_{fDAP}$. The $I_{fDAP}$ at potentials from −90 to −40 mV was obtained by the subtraction method described in Fig. 7. Lowering $[Cl^-]_o$ to 2.5 mM from 125 mM did not affect the amplitude of $I_{fDAP}$ throughout the voltage range.

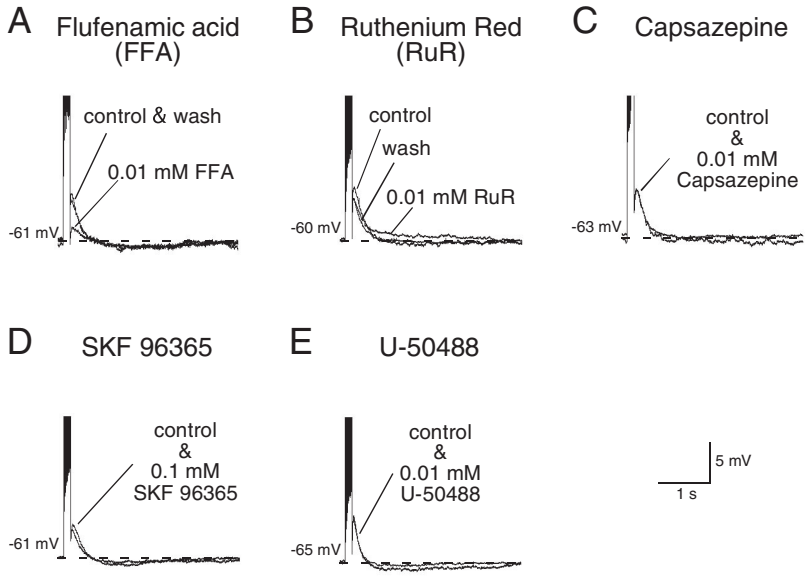


FIG. 10. Effect of the nonselective cation channel blockers on fDAP. The fDAP was generated with a train of spikes during a 200-ms current injection in the presence of extracellular $Cs^+$ and apamin (5 and 100 nM, respectively). The number of spikes evoked was carefully monitored to ensure the same number of spikes (16–20 spikes) were generated before and after any 1 drug application. *A*: $Ca^{2+}$-activated nonselective cation (CAN) channel blocker, FFA, effectively and reversibly blocked the fDAP (n =4). *B*: transient receptor potential (TRP) vanilloid type (TRPV) channel blocker RuR did not effectively reduce the fDAP ($n = 4$). *C*: competitive antagonist of the TRPv1 channel, capsazepine, did not affect the fDAP ($n = 2$). *D*: blocker of TRP canonical type 3 and type 6 channels, SKF 96365, did not affect fDAP ($n = 4$). *E*: dynorphin agonist, U-50488, known to suppress DAPs in MNCs, did not affect the fDAP ($n = 3$).

1987; Smith and Armstrong 1993) or TEA (Greffrath et al. 1998), but they were blocked by external $Cs^+$ (Ghamari-Langroudi and Bourque 1998).

The present study did not suggest the involvement of the $Ca^{2+}$-dependent reduction of a resting $K^+$ conductance in the fDAP. Moreover, neither TTX nor TEA inhibited the fDAP. In fact, TEA enhanced the fDAP (data not shown), possibly because of increased $Ca^{2+}$ influx due to prolonged spike width. In addition, the extracellular application of $Cs^+$ did not block the fDAP. These facts imply that the fDAP has not been clearly examined in MNCs before.

### *Ionic nature of fDAP and possible channels mediating the generation of fDAP in VP neurons*

Our results indicate that $I_{fDAP}$ is generated by $Ca^{2+}$-dependent ion channels that are permeable to $Na^+$ and $K^+$, but not to $Cl^-$. When the *I-V* relationship of the $I_{fDAP}$ was studied, the amplitude of $I_{fDAP}$ increased with hyperpolarization, and a pronounced outward rectification was observed at potential above −50 mV. This rectification was still observed when the cells were filled with a $Cs^+$-gluconate pipette solution that should inhibit the majority of $K^+$ conductances. Despite eliminating these conductances, however, the $I_{fDAP}$ was still present as was its rectification at depolarized potentials. Although a more thorough examination is required before making a conclusion, these findings indicate that the conductance that underlies the $I_{fDAP}$ is probably permeable to intracellular $Cs^+$, and the $I_{fDAP}$ is not only $Ca^{2+}$-dependent but also voltage-dependent. To our knowledge, the only ion channel classes known to meet these criteria are $Ca^{2+}$-activated nonselective cation (CAN) channels.

It has been shown that DAPs and plateau potentials can result from the activation of CAN channels in MNCs (Ghamari-Langroudi and Bourque 2002) as well as in other cell types of mammalian cells. These include neuroblastoma (Yellen 1982), sensory neurons (Razani-Boroujerdi and Partridge 1993), hippocampal CA1 pyramidal neurons (Fraser and MacVicar 1996), prefrontal cortex neurons (Haj-Dahmane and Andrade 1997), dorsal horn neurons (Morisset and Nagy 1999), neocortical cells (Schiller 2004), subthalamic neurons (Zhu et al. 2004, 2005), and olfactory interneurons, Blanes cells (Pressler and Strowbridge 2006). In addition, the plateau potentials and bursting activity mediated by the CAN have been studied to a great extent in invertebrate cells (Hung and Magoski 2007; Kramer and Zucker 1985; Lupinsky and Magoski 2006; Partridge and Swandulla 1987; Swandulla and Lux 1985; Zhang et al. 1995). More importantly, FFA has been reported to effectively block DAPs and/or burst firing in MNCs (Ghamari-Langroudi and Bourque 2002), dorsal horn neurons (Morisset and Nagy 1999), neocortical cells (Schiller 2004), subthalamic neurons (Zhu et al. 2004, 2005), and olfactory interneurons (Pressler and Strowbridge 2006). These facts strongly imply the involvement of CAN channels in generation of fDAP in VP neurons. However, it must be noted that the time course of the fDAP in VP neurons is relatively shorter (several hundreds of milliseconds) compared with some other CAN current-mediated phenomena that last several seconds (Pressler and Strowbridge 2006; Schiller 2004), and, as stated herein, shorter than the sDAP in SON neurons. The time course of the fDAP may also be masked by the onset of the sAHP.

TRPM4 and TRPM5, two closely related members of the TRPM channels are unique among the TRP channel family (Clapham 2007; Montell 2005; Nilius et al. 2007; Venkatachalam and Montell 2007). Unlike other TRP channels that are either $Ca^{2+}$-permeable or even highly $Ca^{2+}$-selective channels, TRPM4 and TRPM5 have no detectable permeability to $Ca^{2+}$ or $Cl^-$ (Hofmann et al. 2003; Launay et al. 2002; Nilius et al. 2003, 2005). Moreover, gating of TRPM4 and TRPM5 is not only regulated by $Ca^{2+}$ but also by transmembrane voltage (Hofmann et al. 2003; Launay et al. 2002; Nilius et al. 2003, 2005). Interestingly, it has been reported that TRPM4 and TRPM5 can be blocked by FFA (Ullrich et al. 2005). All these properties fit well with the results from the present study, thus suggesting the involvement of the TRPM4/5 in expression of the fDAP in VP. However, such a conclusion should be reserved until the development of a more selective antagonist of TRPM4/5 because FFA also inhibits a variety of ion chan-

nels in a range of tissues including the voltage-gated $Na^+$ (Lee et al. 2003) and $K^+$ (Lee and Wang 1999) channels and $Ca^{2+}$-activated chloride currents (Kim et al. 2003). FFA also causes a transient release of intracellular $Ca^{2+}$-release from stores (Partridge and Valenzuela 1999). Moreover, the molecular identification and the biophysical properties of these channels must be elucidated by RT-PCR or a comparable technique, and single channel recordings, respectively.

VP neurons in SON are directly osmosensitive, and this osmosensitivity is mediated by stretch-inhibited cation channels (Oliet and Bourque 1993). A recent study showed that SON neurons express an N-terminal splice variant of the TRP vanilloid type-1 (TRPV1) channel but not full-length TRPV1 (Sharif Naeini et al. 2006). In that study, the SON neurons in TRPV1 knockout mice could not generate increases in membrane conductance in response to hyperosmotic stimulation (Sharif Naeini et al. 2006). Thus the N-terminal splice variant of the TRPV1 has been suggested as a functional stretch-inhibited cation channel (Sharif Naeini et al. 2006). In addition, other studies have indicated that TRPV4 channel may contribute to the detection of osmotic signals (Liedtke et al. 2000; Strotmann et al. 2000) and to the osmotic control of VP release (Liedtke and Friedman 2003; Mizuno et al. 2003). The inorganic polycationic dye, ruthenium red (RuR), appears to be one of the most selective blockers of currents through the TRPV channels (Tominaga et al. 1998) as all TRPV channels are reportedly blocked by RuR (Watanabe et al. 2003). Moreover the increase in membrane conductance provoked by hyperosmolality was significantly attenuated in the presence of RuR in MNCs of mice (Sharif Naeini et al. 2006). In the present study, an application of RuR did not affect the fDAP in VP neurons. This strongly suggests that the currents underlying fDAP are not mediated by TRPV channels and the $I_{fDAP}$ probably plays little role in the osmosensitive activation of VP neurons.

### *Possible functional role of the fDAP in MNCs*

Although the precise physiological functions of the fDAP are unknown at this point, the fact that essentially all VP neurons, whereas only a minority of OT neurons, possess this property implicates the involvement of fDAP in the generation of the specific firing pattern observed in VP neurons. In MNCs, $Ca^{2+}$ influx through high-voltage-gated channels typically evoked by spikes, but not sub-threshold events, is required to generate a plateau potential on which phasic bursts ride (Andrew and Dudek 1984a). Therefore VP neurons require the ability to depolarize from negative potentials to the voltage range where bursts may occur through the activation of the current underlying the sDAP. Thus the fDAP may serve to bootstrap the sDAP, but this would clearly depend on the nature of the interaction between the fDAP and the medium AHP.

The DAPs and phasic bursting activity can be observed in brain slice preparations when synaptic activity has been blocked (Andrew 1987; Bourque and Renaud 1984; Hatton 1982) and even somewhat in dissociated cells (Oliet and Bourque 1992). Therefore phasic bursting is largely an intrinsic property of VP neurons. However, the phasic bursting in vivo is clearly triggered from synaptic inputs because excitatory amino acid receptor antagonists prevent bursts (Brown et al. 2004; Nissen et al. 1994). Therefore phasic bursts in MNCs are not intrinsically regenerative in vivo. This discrepancy may be due to the steep voltage sensitivity of the sDAP. Phasic firing in vitro is observed only within a relatively narrow range of membrane potential (−48 to −55 mV). Slightly more depolarized potentials results in continuous firing, whereas a slightly hyperpolarized potentials results in slow irregular firing or no firing at all (Inenaga et al. 1993). In contrast, most VP neurons in vivo exhibit a slow irregular discharge in absence of stimulation (Wakerley et al. 1978), suggesting the resting potential in vivo is below the range of sDAP activation. This probably prevents excessive firing that would result in inappropriate hormone secretion at rest. The fDAP may also be needed for the initiation of bursting to occur appropriately in response to strong excitatory synaptic inputs from osmosensitive areas (Denton et al. 1996; McKinley et al. 1996; Richard and Bourque 1995) in response to osmotic challenge. Interestingly, it has been shown that *N*-methyl-D-aspatate (NMDA) induced burst via activation of CAN current in subthalamic neurons (Zhu et al. 2004) and in neocortical cells (Schiller 2004). In addition, $Ca^{2+}$ influx responsible for activation of CAN current was mediated by both NMDA-receptor channels and voltage-gated calcium channels and to lesser extent internal calcium stores (Schiller 2004). These reports further support the notion in the synaptic activation of the fDAP in VP neurons. Indeed, NMDA receptor activation in SON neurons also contributes to rhythmic burst firing (Hu and Bourque 1992). Therefore we suggest that the $Ca^{2+}$-activated fDAP plays a role in the instigation of phasic firing, the latter relying in turn on the subsequent activation of the sDAP.

## ACKNOWLEDGMENTS

The authors thank Dr. R. C. Foehring for reading earlier versions of this manuscript and P. K. Tripathi for technical assistance.

## GRANTS

This study was supported by National Institutes of Health Grants R03 HD-45634 to R. Teruyama and R01 NS-23941 to W. E. Armstrong.

## REFERENCES

**Andrew RD.** Endogenous bursting by rat supraoptic neuroendocrine cells is calcium dependent. *J Physiol* 384: 451–465, 1987.

**Andrew RD, Dudek FE.** Burst discharge in mammalian neuroendocrine cells involves an intrinsic regenerative mechanism. *Science* 221: 1050–1052, 1983.

**Andrew RD, Dudek FE.** Analysis of intracellularly recorded phasic bursting by mammalian neuroendocrine cells. *J Neurophysiol* 51: 552–566, 1984a.

**Andrew RD, Dudek FE.** Intrinsic inhibition in magnocellular neuroendocrine cells of rat hypothalamus. *J Physiol* 353: 171–185, 1984b.

**Armstrong WE, Smith BN, Tian M.** Electrophysiological characteristics of immunochemically identified rat oxytocin and vasopressin neurones in vitro. *J Physiol* 475: 115–128, 1994.

**Boulay G, Zhu X, Peyton M, Jiang M, Hurst R, Stefani E, Birnbaumer L.** Cloning and expression of a novel mammalian homolog of *Drosophila* transient receptor potential (Trp) involved in calcium entry secondary to activation of receptors coupled by the Gq class of G protein. *J Biol Chem* 272: 29672–29680, 1997.

**Bourque CW, Brown DA.** Apamin and d-tubocurarine block the afterhyperpolarization of rat supraoptic neurosecretory neurons. *Neurosci Lett* 82: 185–190, 1987.

**Bourque CW, Renaud LP.** Activity patterns and osmosensitivity of rat supraoptic neurones in perfused hypothalamic explants. *J Physiol* 349: 631–642, 1984.

**Brimble MJ, Dyball RE.** Characterization of the responses of oxytocin- and vasopressin-secreting neurons in the supraoptic nucleus to osmotic stimulation. *J Physiol* 271: 253–271, 1977.

**Brown CH, Bourque CW.** Autocrine feedback inhibition of plateau potentials terminates phasic bursts in magnocellular neurosecretory cells of the rat supraoptic nucleus. *J Physiol* 557: 949–960, 2004.

**Brown CH, Bull PM, Bourque CW.** Phasic bursts in rat magnocellular neurosecretory cells are not intrinsically regenerative in vivo. *Eur J Neurosci* 19: 2977–2983, 2004.

**Brown CH, Ghamari-Langroudi M, Leng G, Bourque CW.** Kappa-opioid receptor activation inhibits post-spike depolarizing after-potentials in rat supraoptic nucleus neurones in vitro. *J Neuroendocrinol* 11: 825–828, 1999.

**Cazalis M, Dayanithi G, Nordmann JJ.** The role of patterned burst and interburst interval on the excitation-coupling mechanism in the isolated rat neural lobe. *J Physiol* 369: 45–60, 1985.

**Clapham DE.** SnapShot: mammalian TRP channels. *Cell* 129: 220, 2007.

**Clapham DE, Runnels LW, Strubing C.** The TRP ion channel family. *Nat Rev Neurosci* 2: 387–396, 2001.

**Denton DA, McKinley MJ, Weisinger RS.** Hypothalamic integration of body fluid regulation. *Proc Natl Acad Sci USA* 93: 7397–7404, 1996.

**Dickenson AH, Dray A.** Selective antagonism of capsaicin by capsazepine: evidence for a spinal receptor site in capsaicin-induced antinociception. *Br J Pharmacol* 104: 1045–1049, 1991.

**Dutton A, Dyball REJ.** Phasic firing enhances vasopressin release from the rat neurohypophysis. *J Physiol* 290: 443–440, 1979.

**Foehring RC, Armstrong WE.** Pharmacological dissection of high-voltage-activated $Ca^{2+}$ current types in acutely dissociated rat supraoptic magnocellular neurons. *J Neurophysiol* 76: 977–983, 1996.

**Fraser DD, MacVicar BA.** Cholinergic-dependent plateau potential in hippocampal CA1 pyramidal neurons. *J Neurosci* 16: 4113–4128, 1996.

**Ghamari-Langroudi M, Bourque CW.** Caesium blocks depolarizing afterpotentials and phasic firing in rat supraoptic neurons. *J Physiol* 510: 165–175, 1998.

**Ghamari-Langroudi M, Bourque CW.** Flufenamic acid blocks depolarizing afterpotentials and phasic firing in rat supraoptic neurons. *J Physiol* 545: 537–542, 2002.

**Ghamari-Langroudi M, Bourque CW.** Muscarinic receptor modulation of slow afterhyperpolarization and phasic firing in rat supraoptic nucleus neurons. *J Neurosci* 24: 7718–7726, 2004.

**Greffrath W, Martin E, Reuss S, Boehmer G.** Components of afterhyperpolarization in magnocellular neurons of the rat supraoptic nucleus in vitro. *J Physiol* 513: 493–506, 1998.

**Haj-Dahmane S, Andrade R.** Calcium-activated cation nonselective current contributes to the fast afterdepolarization in rat prefrontal cortex neurons. *J Neurophysiol* 78: 1983–1989, 1997.

**Harris MC, Dreifuss J-J, Legros J-J.** Excitation of phasically firing supraoptic neurones during vasopressin release. *Nature* 258: 80–82, 1975.

**Hartzell C, Putzier I, Arreola J.** Calcium-activated chloride channels. *Annu Rev Physiol* 67: 719–758, 2005.

**Hatton GI.** Phasic bursting activity of rat paraventricular neurons in the absence of synaptic transmission. *J Physiol* 327: 273–284, 1982.

**Hofmann T, Chubanov V, Gudermann T, Montell C.** TRPM5 is a voltage-modulated and Ca(2+)-activated monovalent selective cation channel. *Curr Biol* 13: 1153–1158, 2003.

**Hu B, Bourque CW.** NMDA receptor-mediated rhythmic bursting activity in rat supraoptic nucleus neurons in vitro. *J Physiol* 458: 667–687, 1992.

**Hung AY, Magoski NS.** Activity-dependent initiation of a prolonged depolarization in *Aplysia* bag cell neurons: role for a cation channel. *J Neurophysiol* 97: 2465–2479, 2007.

**Inenaga K, Nagatomo T, Kannan H, Yamashita H.** Inward sodium current involvement in regenerative bursting activity of rat magnocellular supraoptic neurons in vitro. *J Physiol* 465: 289–301, 1993.

**Inoue R, Okada T, Onoue H, Hara Y, Shimizu S, Naitoh S, Ito Y, Mori Y.** The transient receptor potential protein homologue TRP6 is the essential component of vascular alpha(1)-adrenoceptor-activated Ca(2+)-permeable cation channel. *Circ Res* 88: 325–332, 2001.

**Kim SJ, Shin SY, Lee JE, Kim JH, Uhm DY.** $Ca^{2+}$-activated $Cl^-$ channel currents in rat ventral prostate epithelial cells. *Prostate* 55: 118–127, 2003.

**Kirkpatrick K, Bourque CW.** Activity dependence and functional role of the apamin-sensitive $K^+$ current in rat supraoptic neurons in vitro. *J Physiol* 494: 389–398, 1996.

**Kramer RH, Zucker RS.** Calcium-dependent inward current in *Aplysia* bursting pace-maker neurons. *J Physiol* 362: 107–130, 1985.

**Launay P, Fleig A, Perraud AL, Scharenberg AM, Penner R, Kinet JP.** TRPM4 is a $Ca^{2+}$-activated nonselective cation channel mediating cell membrane depolarization. *Cell* 109: 397–407, 2002.

**Lee HM, Kim HI, Shin YK, Lee CS, Park M, Song JH.** Diclofenac inhibition of sodium currents in rat dorsal root ganglion neurons. *Brain Res* 992: 120–127, 2003.

**Lee YT, Wang Q.** Inhibition of hKv2.1, a major human neuronal voltage-gated $K^+$ channel, by meclofenamic acid. *Eur J Pharmacol* 378: 349–356, 1999.

**Li Z, Hatton GI.** $Ca^{2+}$ release from internal stores: role in generating depolarizing afterpotentials in rat supraoptic neurons. *J Physiol* 498: 339–350, 1997a.

**Li Z, Hatton GI.** Reduced outward $K^+$ conductances generate depolarizing afterpotentials in rat supraoptic nucleus neurons. *J Physiol* 505: 95–106, 1997b.

**Liedtke W, Choe Y, Marti-Renom MA, Bell AM, Denis CS, Sali A, Hudspeth AJ, Friedman JM, Heller S.** Vanilloid receptor-related osmotically activated channel (VR-OAC), a candidate vertebrate osmoreceptor. *Cell* 103: 525–535, 2000.

**Liedtke W, Friedman JM.** Abnormal osmotic regulation in trpv4-/- mice. *Proc Natl Acad Sci USA* 100: 13698–13703, 2003.

**Lupinsky DA, Magoski NS.** $Ca^{2+}$-dependent regulation of a non-selective cation channel from *Aplysia* bag cell neurons. *J Physiol* 575: 491–506, 2006.

**McKinley MJ, Pennington GL, Oldfield BJ.** Anteroventral wall of the third ventricle and dorsal lamina terminalis: headquarters for control of body fluid homeostasis? *Clin Exp Pharmacol Physiol* 23: 271–281, 1996.

**Mizuno A, Matsumoto N, Imai M, Suzuki M.** Impaired osmotic sensation in mice lacking TRPV4. *Am J Physiol Cell Physiol* 285: C96–101, 2003.

**Montell C.** The TRP superfamily of cation channels. *Sci STKE* 2005: re3, 2005.

**Montell C, Birnbaumer L, Flockerzi V, Bindels RJ, Bruford EA, Caterina MJ, Clapham DE, Harteneck C, Heller S, Julius D, Kojima I, Mori Y, Penner R, Prawitt D, Scharenberg AM, Schultz G, Shimizu N, Zhu MX.** A unified nomenclature for the superfamily of TRP cation channels. *Mol Cell* 9: 229–231, 2002.

**Morisset V, Nagy F.** Ionic basis for plateau potentials in deep dorsal horn neurons of the rat spinal cord. *J Neurosci* 19: 7309–7316, 1999.

**Nilius B, Owsianik G, Voets T, Peters JA.** Transient receptor potential cation channels in disease. *Physiol Rev* 87: 165–217, 2007.

**Nilius B, Prenen J, Droogmans G, Voets T, Vennekens R, Freichel M, Wissenbach U, Flockerzi V.** Voltage dependence of the $Ca^{2+}$-activated cation channel TRPM4. *J Biol Chem* 278: 30813–30820, 2003.

**Nilius B, Prenen J, Janssens A, Owsianik G, Wang C, Zhu MX, Voets T.** The selectivity filter of the cation channel TRPM4. *J Biol Chem* 280: 22899–22906, 2005.

**Nissen R, Hu B, Renaud LP.** N-methyl-D-aspartate receptor antagonist ketamine selectively attenuates spontaneous phasic activity of supraoptic vasopressin neurons in vivo. *Neuroscience* 59: 115–120, 1994.

**Oliet SH, Bourque CW.** Properties of supraoptic magnocellular neurones isolated from the adult rat. *J Physiol* 455: 291–306, 1992.

**Oliet SH, Bourque CW.** Mechanosensitive channels transduce osmosensitivity in supraoptic neurons. *Nature* 364: 341–343, 1993.

**Partridge LD, Swandulla D.** Single Ca-activated cation channels in bursting neurons of Helix. *Pfluegers* 410: 627–631, 1987.

**Partridge LD, Valenzuela CF.** $Ca^{2+}$ store-dependent potentiation of $Ca^{2+}$-activated non-selective cation channels in rat hippocampal neurones in vitro. *J Physiol* 521 Pt 3: 617–627, 1999.

**Perez CA, Huang L, Rong M, Kozak JA, Preuss AK, Zhang H, Max M, Margolskee RF.** A transient receptor potential channel expressed in taste receptor cells. *Nat Neurosci* 5: 1169–1176, 2002.

**Poulain DA, Wakerley JB.** Electrophysiology of hypothalamic magnocellular neurons secreting oxytocin and vasopressin. *Neuroscience* 7: 773–808, 1982.

**Pressler RT, Strowbridge BW.** Blanes cells mediate persistent feedforward inhibition onto granule cells in the olfactory bulb. *Neuron* 49: 889–904, 2006.

**Razani-Boroujerdi S, Partridge LD.** Activation and modulation of calcium-activated non-selective cation channels from embryonic chick sensory neurons. *Brain Res* 623: 195–200, 1993.

**Richard D, Bourque CW.** Synaptic control of rat supraoptic neurons during osmotic stimulation of the organum vasculosum lamina terminalis in vitro. *J Physiol* 489: 567–577, 1995.

**Rohacs T, Lopes CM, Michailidis I, Logothetis DE.** PI(4,5)P2 regulates the activation and desensitization of TRPM8 channels through the TRP domain. *Nat Neurosci* 8: 626–634, 2005.

**Schiller Y.** Activation of a calcium-activated cation current during epileptiform discharges and its possible role in sustaining seizure-like events in neocortical slices. *J Neurophysiol* 92: 862–872, 2004.

**Sharif Naeini R, Witty MF, Seguela P, Bourque CW.** An N-terminal variant of Trpv1 channel is required for osmosensory transduction. *Nat Neurosci* 9: 93–98, 2006.

**Smith BN, Armstrong WE.** Histamine enhances the depolarizing afterpotential of immunohistochemically identified vasopressin neurons in the rat supraoptic nucleus via H1-receptor activation. *Neuroscience* 53: 855–864, 1993.

**Stern JE, Armstrong WE.** Changes in the electrical properties of supraoptic nucleus oxytocin and vasopressin neurons during lactation. *J Neurosci* 16: 4861–4871, 1996.

**Strotmann R, Harteneck C, Nunnenmacher K, Schultz G, Plant TD.** OTRPC4, a nonselective cation channel that confers sensitivity to extracellular osmolarity. *Nat Cell Biol* 2: 695–702, 2000.

**Swandulla D, Lux HD.** Activation of a nonspecific cation conductance by intracellular $Ca^{2+}$ elevation in bursting pacemaker neurons of Helix pomatia. *J Neurophysiol* 54: 1430–1443, 1985.

**Teruyama R, Armstrong WE.** Changes in the active membrane properties of rat supraoptic neurons during pregnancy and lactation. *J Neuroendocrinol* 14: 933–944, 2002.

**Teruyama R, Armstrong WE.** Enhancement of calcium-dependent afterpotentials in oxytocin neurons of the rat supraoptic nucleus during lactation. *J Physiol* 566: 505–518, 2005a.

**Teruyama R**, **Armstrong WE.** Calcium-dependent fast and slow depolarizing afterpotentials in oxytocin and vasopressin neurons in the supraoptic nucleus. *Soc Neurosci Abstrt* 993: 16, 2005b.

**Teruyama R**, **Armstrong WE.** Characterization of the fast depolarizing after-potential in vasopressin neurons in the supraoptic nucleus. *Soc Neurosci Abstr* 153: 8, 2006.

**Tominaga M, Caterina MJ, Malmberg AB, Rosen TA, Gilbert H, Skinner K, Raumann BE, Basbaum AI, Julius D.** The cloned capsaicin receptor integrates multiple pain-producing stimuli. *Neuron* 21: 531–543, 1998.

**Tseng PH, Lin HP, Hu H, Wang C, Zhu MX, Chen CS.** The canonical transient receptor potential 6 channel as a putative phosphatidylinositol 3,4,5-trisphosphate-sensitive calcium entry system. *Biochemistry* 43: 11701–11708, 2004.

**Ullrich ND, Voets T, Prenen J, Vennekens R, Talavera K, Droogmans G, Nilius B.** Comparison of functional properties of the $Ca^{2+}$-activated cation channels TRPM4 and TRPM5 from mice. *Cell Calcium* 37: 267–278, 2005.

**Venkatachalam K, Montell C.** TRP channels. *Annu Rev Biochem* 76: 387–417, 2007.

**Wainwright A, Rutter AR, Seabrook GR, Reilly K, Oliver KR.** Discrete expression of TRPV2 within the hypothalamo-neurohypophysial system: implications for regulatory activity within the hypothalamic-pituitary-adrenal axis. *J Comp Neurol* 474: 24–42, 2004.

**Wakerley JB, Poulain DA, Brown D.** Comparison of firing patterns in oxytocin- and vasopressin-releasing neurones during progressive dehydration. *Brain Res* 148: 425–440, 1978.

**Watanabe H, Vriens J, Prenen J, Droogmans G, Voets T, Nilius B.** Anandamide and arachidonic acid use epoxyeicosatrienoic acids to activate TRPV4 channels. *Nature* 424: 434–438, 2003.

**Xu XZ, Moebius F, Gill DL, Montell C.** Regulation of melastatin, a TRP-related protein, through interaction with a cytoplasmic isoform. *Proc Natl Acad Sci USA* 98: 10692–10697, 2001.

**Yellen G.** Single $Ca^{2+}$-activated nonselective cation channels in neuroblastoma. *Nature* 296: 357–359, 1982.

**Zhang B, Wootton JF, Harris-Warrick RM.** Calcium-dependent plateau potentials in a crab stomatogastric ganglion motor neuron. II. Calcium-activated slow inward current. *J Neurophysiol* 74: 1938–1946, 1995.

**Zhu X, Jiang M, Birnbaumer L.** Receptor-activated $Ca^{2+}$ influx via human Trp3 stably expressed in human embryonic kidney (HEK)293 cells. Evidence for a non-capacitative $Ca^{2+}$ entry. *J Biol Chem* 273: 133–142, 1998.

**Zhu ZT, Munhall A, Shen KZ, Johnson SW.** Calcium-dependent subthreshold oscillations determine bursting activity induced by *N*-methyl-D-aspartate in rat subthalamic neurons in vitro. *Eur J Neurosci* 19: 1296–1304, 2004.

**Zhu ZT, Munhall A, Shen KZ, Johnson SW.** NMDA enhances a depolarization-activated inward current in subthalamic neurons. *Neuropharmacology* 49: 317–327, 2005.